S-Oxygenation of Thiocarbamides I: Oxidation of Phenylthiourea by Chlorite in Acidic Media

Tabitha R. Chigwada,† Edward Chikwana, and Reuben H. Simoyi*

Department of Chemistry, Portland State University, Portland, Oregon 97207-0751

Received: September 13, 2004; In Final Form: November 19, 2004

The oxidation of 1-phenyl-2-thiourea (PTU) by chlorite was studied in aqueous acidic media. The reaction is extremely complex with reaction dynamics strongly influenced by the pH of reaction medium. In excess chlorite concentrations the reaction stoichiometry involves the complete desulfurization of PTU to yield a urea residue and sulfate: $2ClO_2^- + PhN(H)CSNH_2 + H_2O \rightarrow SO_4^{2-} + PhN(H)CONH_2 + 2Cl^- + 2H^+$. In excess PTU, mixtures of sulfinic and sulfonic acids are formed. The reaction was followed spectrophotometrically by observing the formation of chlorine dioxide which is formed from the reaction of the reactive intermediate HOCl and chlorite: $2ClO_2^- + HOCl + H^+ \rightarrow 2ClO_2(aq) + Cl^- + H_2O$. The complexity of the ClO_2^- − PTU reaction arises from the fact that the reaction of ClO_2 with PTU is slow enough to allow the accumulation of ClO_2 in the presence of PTU. Hence the formation of ClO_2 was observed to be oligooscillatory with transient formation of ClO_2 even in conditions of excess oxidant. The reaction showed complex acid dependence with acid catalysis in pH conditions higher than pK_a of $HClO_2$ and acid retardation in pH conditions of less than 2.0. The rate of oxidation of PTU was given by $-d[PTU]/dt = k_1[ClO_2^-][PTU] + k_2[HClO_2][PTU]$ with the rate law: $-d[PTU]/dt = [Cl(III)]_T[PTU]_0/K_{a1} + [H^+]\,[k_1K_{a1} + k_2[H^+]]$; where $[Cl(III)]_T$ is the sum of chlorite and chlorous acid and K_{a1} is the acid dissociation constant for chlorous acid. The following bimolecular rate constants were evaluated; $k_1 = 31.5 \pm 2.3\ M^{-1}\ s^{-1}$ and $k_2 = 114 \pm 7\ M^{-1}\ s^{-1}$. The direct reaction of ClO_2 with PTU was autocatalytic in low acid concentrations with a stoichiometric ratio of 8:5; $8ClO_2 + 5PhN(H)CSNH_2 + 9H_2O \rightarrow 5SO_4^{2-} + 5PhN(H)CONH_2 + 8Cl^- + 18H^+$. The proposed mechanism implicates HOCl as a major intermediate whose autocatalytic production determined the observed global dynamics of the reaction. A comprehensive 29-reaction scheme is evoked to describe the complex reaction dynamics.

Introduction

Sulfur compounds undergo a variety of metabolic reactions, namely oxidations, reductions, hydrolysis and conjugations.[1] Sulfur in most organic configurations is nucleophilic, and nucleophilic atoms are usually susceptible to metabolic oxidation.[2] The oxidation of sulfur-containing compounds represents an important aspect of sulfur metabolism. Oxidations of sulfur compounds appear to be involved in many cellular functions, which include the reductive degradation of polypeptide hormones and proteins, regulation of protein synthesis, maintenance of intracellular redox potential, and protection of the cell from oxidative damage.[3]

The molecular basis for S-oxygenation of sulfur compounds is not well understood since relatively few studies have addressed this problem. Although S-oxygenation of organosulfur xenobiotics by microsomes supplemented with NADPH and oxygen has been extensively studied, the facile oxidations of sulfur compounds by hydrogen peroxide and other species of reduced oxygen, such as superoxide ion, have not received the same attention. In general, the metabolism of sulfur-based xenobiotics such as thionicotinamide[4] and thiobenzamide[5−7] is mediated by enzyme catalysis, with both the microsomal cytochrome P-450 system and the flavin-containing monooxygenases[8−10] playing a role.

It was reported in a 1961 publication that phenylthiourea is extremely toxic to rats but that diphenylthiourea was not.[11] There was and has never been a justification why such physiological differences exist in very similar compounds. No doubt the metabolic pathways of the two compounds must be different, but how, and why?

Subtle differences in substituted thioureas can impart vastly different degrees of toxicity. For example, while α-naphthylthiourea (ANTU) produces pulmonary edema and pleural effusion in rats, its oxidation gives α-naphthylurea, an innocuous substance to rats.[12] Toxicity and tumorigenicity of α-naphthylthiourea can then be evaluated from these experimental data. The possibilities are limited to either the parent compound, metabolic intermediates, or the sulfur-based leaving groups. The toxicity can be narrowed down to only these few processes and compounds.

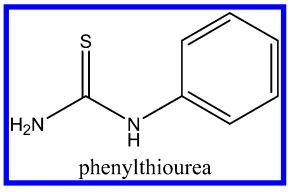

phenylthiourea

We report, in this manuscript, on the oxidation of phenylthiourea by chlorite in acidic medium. The aim of this study was to evaluate the mechanism, products, and intermediates formed in this oxidation. The S-oxygenation mechanism of phenyl-

* Corresponding author.
† Permanent address: Department of Chemistry, West Virginia University, Morgantown, WV 26506-6045.

10.1021/jp0458654 CCC: $30.25
Published on Web 01/26/2005

thiourea by chlorite would contribute greatly to the possible elucidation of its metabolic activation. Phenylthiourea contains the thiocarbamide group that is responsible for goitrogenic activity[9,13] in methimazole[14] and 6-propyl-2-thiouracil.[15] Its use as a goitrogenic was discontinued due to its strong toxicological side effects.[16,17] Of special interest is the fate of the C−S bond after the full oxidation of PTU. Its cleavage, or lack of, would give us a better insight into the speculation of a possible mechanism for its toxicity.

Experimental Section

Materials. The following analytical grade chemicals were used without any further purification: perchloric acid (72%), 1-phenyl-2-thiourea, PTU (Acros), sodium perchlorate (Fisher), and barium chloride (Aldrich). Commercially available sodium chlorite (Aldrich) varied in purity (78−88%) with the main impurities being chloride and carbonate. The sodium chlorite was recrystallized once from a water/ethanol/acetone mixture to bring the assay value to approximately 96%. The recrystallized chlorite was standardized iodometrically by adding excess acidified potassium iodide and titrating liberated iodine against sodium thiosulfate with freshly prepared starch as an indicator.[18] Chlorine dioxide was prepared by the standard method of oxidizing potassium chlorate in acidic medium.[19] The aqueous chlorine dioxide was stored in an acidic medium in a volumetric flask wrapped in aluminum foil at 4EC. The chlorine dioxide was then standardized iodometrically and results obtained were also confirmed spectrophotometrically by using a molar absorptivity coefficient of 1265 M^{-1} cm^{-1} at 360 nm on a Perkin-Elmer Lambda 2S UV/Vis spectrophotometer.[20]

Tests for Adventitious Metal Ion Catalysis. Recent work by Doona et al. showed adventitious metal ions catalysis in reductions involving thiourea.[21] It was important to eliminate the possibility for such catalysis in the chlorite−PTU system. Water used for preparing reagent solutions was obtained from a Barnstead Sybron Corporation water purification unit capable of producing both distilled and deionized water (Nanopure). Not much difference was observed in the general reaction kinetics observed with distilled and deionized water. We utilized inductively-coupled plasma mass spectrometry (ICPMS) to quantitatively evaluate the concentrations of a number of metal ions in the water used for our reaction medium. ICPMS analysis showed negligible concentrations of iron, copper, and silver and approximately 1.5 ppb of cadmium and 0.43 ppb in lead. Reactions run with metal ion chelators such as EDTA and deferroxamine did not offer different kinetics and dynamics.

Methods. All experiments were carried out at 25±0.5 °C (Neslab thermostat bath) and an ionic strength of 1.0 M (sodium perchlorate). The ClO_2^-, ClO_2/PTU reactions were monitored spectrophotometrically at $\lambda = 360$ nm as reactions were performed in excess chlorite so as to utilize the formation of chlorine dioxide as an indicator of the extent of the reaction. These reactions were also concurrently monitored at 249 nm, which is the absorption peak for phenylthiourea. Figure 1a shows superimposed UV spectra of the three major reagents in the reaction mixture: phenylthiourea ($\lambda_{max} = 249$ nm, $\epsilon_{max} = 12\,312$ M^{-1} cm^{-1}), phenylurea ($\lambda_{max} = 235$ nm, $\epsilon_{max} = 37\,180$ M^{-1} cm^{-1}), and chlorine dioxide ($\lambda_{max} = 360$ nm, $\epsilon_{max} = 1265$ M^{-1} cm^{-1}). The absorptivity coefficient of chlorine dioxide at 249 nm was 130 M^{-1} cm^{-1} while both phenylthiourea and phenylurea had negligible contributions to the absorbances observed at 360 nm. Kinetics measurements were performed on a Hi-Tech Scientific SF61-DX2 double-mixing stopped-flow spectrophotometer. The data from the spectrophotometer were amplified and digitized via an Omega Engineering DAS-50/1 16-bit A/D board interfaced to a Pentium IV computer for storage and data analysis. Stoichiometric determinations were carried out by mixing various ratios of chlorite and PTU in stoppered volumetric flasks and scanning them spectrophotometrically for formation of ClO_2 and depletion of PTU after an incubation period of up to 2 days. Qualitative and quantitative analysis of sulfate was performed through its precipitation as $BaSO_4$. For reactions run in excess chlorite conditions, the excess chlorite oxidizing power was evaluated by addition of excess acidified iodide which was titrated against standard thiosulfate with freshly prepared starch as indicator. The thiosulfate titer was next plotted against the amount of chlorite used and this plot was extrapolated to zero titer to obtain the stoichiometry of the reaction.

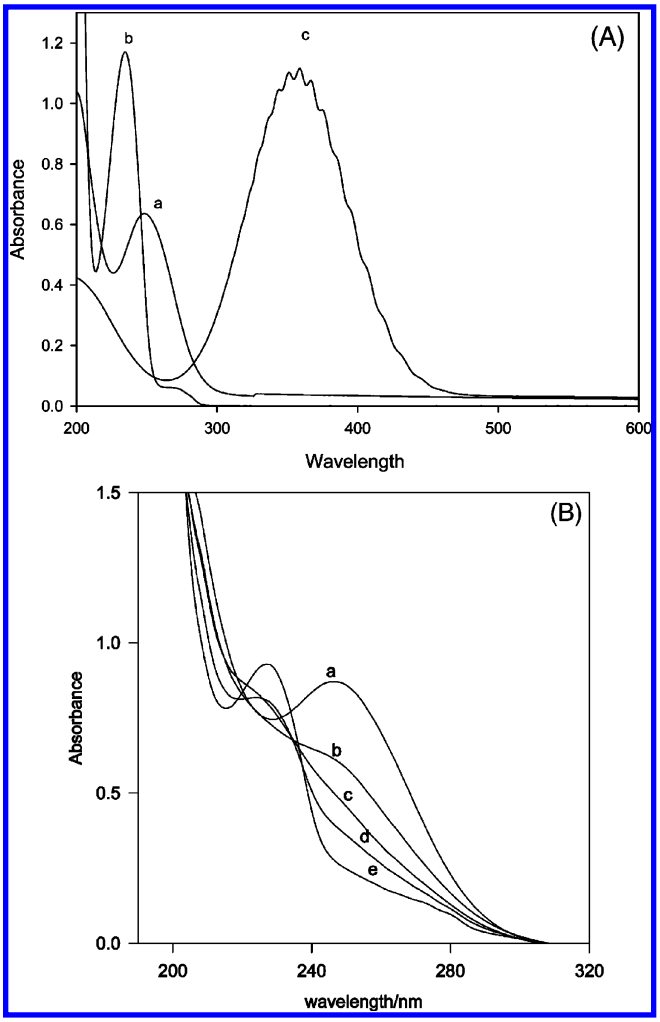

Figure 1. (A) Three superimposed spectra of (a) 5×10^{-5} M phenylthiourea (reductant), (b) 1×10^{-5} M phenylurea (product), and (c) 8.8×10^{-4} M chlorine dioxide (product) showing peaks at 248, 235, and 360 nm, respectively. Phenylurea has a reasonably high absorptivity coefficient at 249 nm (λ_{max} for phenylthiourea). At the beginning of the reaction, however, all absorbance activity observed at 249 nm will be due to the depletion of phenylthiourea. There is no interference from substrate or product at 360 nm. (B) Spectral scans of reagent solutions containing phenylthiourea and varying concentrations of chlorite between 200 and 350 nm. PTU has a well-defined peak at 249 nm which progressively diminishes with increasing chlorite concentrations. At chlorite-to-phenylthiourea ratios greater than 2.0 a chlorine dioxide peak is observed at 360 nm after a short induction period. $[PTU]_0 = 5.0 \times 10^{-4}$ M, $[H^+]_0 = 0.125$ M, $[ClO_2^-]_0 =$ (a) 2.5×10^{-5} M, (b) 5.0×10^{-5} M, (c) 1.0×10^{-4} M, (d) 2.0×10^{-4} M, and (e) 3.5×10^{-4} M.

Synthesis of Phenylthiourea Dioxide (N-Phenylaminoiminomethanesulfinic Acid).[22] Exactly 0.02 mol of PTU with 0.07 mol of molybdenyl acetylacetonate was dissolved in a 40−60 mixture of ether and dioxane and was carefully and slowly added to 2 equiv of hydrogen peroxide with continuous stirring at −15 °C. This mixture was allowed to stand for an hour at room temperature and then left overnight at −4 °C. After thawing, some off-white powdery crystals were obtained which could be washed with acetonitrile. These phenylthiourea dioxide crystals were vacuum-dried and kept in the dark and cold until they were ready for use.

Results

Stoichiometry. The reaction involved successive oxidation of the sulfur center to sulfate and a urea residue:

$$2ClO_2^- + PhN(H)CSNH_2 + H_2O \rightarrow SO_4^{2-} + PhN(H)CONH_2 + 2Cl^- + 2H^+ \quad (R1)$$

Stoichiometry R1 was achieved in conditions of excess chlorite; with an oxidant-to-reductant ratio, $R = [ClO_2^-]_0/[PTU]_0 \geq 2.0$ and after prolonged incubation of the reaction solutions. The stoichiometry was also evaluated spectrophotometrically by observing the absorption peak of PTU at 249 nm and the chlorine dioxide peak at 360 nm. Figure 1b shows a series of spectra taken at various ratios of chlorite to PTU. Successive increases in chlorite concentrations for fixed $[PTU]_0$ showed a gradual decrease in this peak until it attained some baseline absorbance from the product, phenylurea. Spectrum e in Figure 1b is the same as that of phenylurea (spectrum b) in Figure 1a. Chlorite concentrations in excess of that required by stoichiometry R1 gave chlorine dioxide as a product, and this could be detected by its absorption peak at 360 nm. Qualitatively, it could be detected by the deep blue-black coloration it gave with starch prepared with mercuric iodide. Contrary to other oxyhalogen oxidations,[23] the chlorine dioxide formed could not be utilized for stoichiometric determinations because the excess chlorite slowly decomposed in acidic media over several days to give chlorine dioxide which could not be related to the initial amount of PTU:[24]

$$5ClO_2^- + 4H^+ \rightarrow 4ClO_2(aq) + 2H_2O + Cl^- \quad (R2)$$

Iodometric techniques, however, were utilized in order to evaluate the excess oxidizing power in conditions of excess chlorite. The analyses gave a stoichiometric ratio slightly greater than the 2:1 given in reaction R1, especially in low acid conditions. This could be attributed to the reaction of chlorite with HOCl to give inert chlorate[25,26]:

$$ClO_2^- + HOCl \rightarrow ClO_3^- + Cl^- + H^+ \quad (R3)$$

Pathway R3 is insignificant in highly acidic environments where reaction R2 is dominant.[27] Although reaction R3 deactivated some oxychlorine species, reaction R2, however, does not alter the overall oxidizing power of the product solution, and iodometric techniques could still be able to evaluate the excess ClO_2^-. The stoichiometry of the chlorine dioxide−PTU reaction was experimentally determined to be

$$8ClO_2 + 5PhN(H)CSNH_2 + 9H_2O \rightarrow 5SO_4^{2-} + 5PhN(H)CONH_2 + 8Cl^- + 18H^+ \quad (R4)$$

This stoichiometry was derived spectrophotometrically as well as by iodometric and titrimetric techniques. Stoichiometry R4, however, was obtained after prolonged incubation periods of up to 48 h.

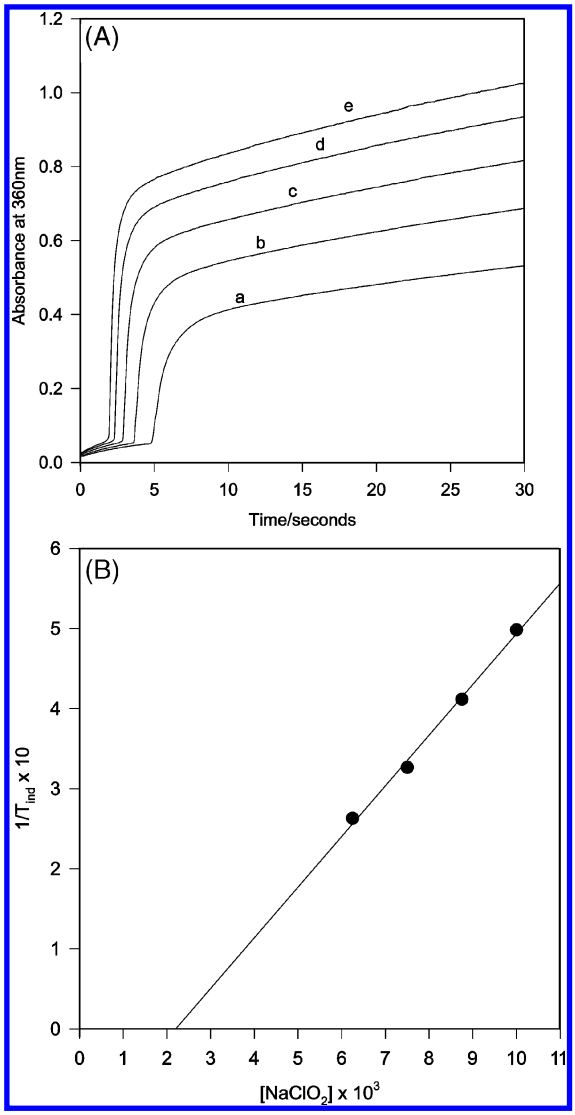

Figure 2. (A) General absorbance traces at 360 nm of the reaction in excess chlorite ($[ClO_2^-]_0/[PTU]_0 > 4.00$). The reaction starts with a short induction period followed by rapid formation of chlorine dioxide. $[PTU]_0 = 1.25 \times 10^{-3}$ M, $[H^+]_0 = 0.125$ M, $[ClO_2^-]_0 =$ (a) 5.0×10^{-3}M, (b) 6.25×10^{-3} M, (c) 7.5×10^{-3} M, (d) 8.75×10^{-3} M, and (e) 1.0×10^{-2} M. (B) Effect of chlorite on the induction period. An inverse relationship also exists for a wide range of chlorite concentrations. $[PTU]_0 = 1.25 \times 10^{-3}$ M, $[H^+]_0 = 0.125$ M. Note that the intercept on the chlorite concentration axis (2.38×10^{-3} M), which represents chlorite concentrations needed to consume PTU, confirms stoichiometry R1 within limits of experimental error (theoretically, 2.5×10^{-3} M needed to consume 1.25×10^{-3} M).

Reaction Kinetics. The reaction dynamics were extremely complex, with a highly complex dependence on the pH of the reaction environment. The reaction dynamics were less complex in conditions of high excess chlorite, in which the oxidant-to-reductant ratio, $R \geq 4$, and in high acid concentrations, $[H^+]_0 \geq 0.10$ M. Under these conditions the reaction showed a clean induction period before formation of chlorine dioxide. Figure 2a shows such traces at 360 nm. The rate of formation of chlorine dioxide after the induction period is directly proportional to the chlorite concentrations. There is an inverse dependence of the induction period to the initial chlorite concentrations (see Figure 2b). This appears to indicate that

chlorite is involved in the reaction kinetics that consumes PTU to the first power. The plot in Figure 2b was also utilized to evaluate reaction stoichiometry R1. By extrapolating to $T_{ind} = \infty$ ($1/T_{Ind} = 0$), one can evaluate the minimum amount of $[ClO_2^-]_0$ needed to produce ClO_2(aq) as a product. This was after assuming that with $[ClO_2^-]_0$ less than that needed for stoichiometry R1, no chlorine dioxide would be formed. The data in Figure 2b show that, with $[PTU]_0 = 0.00125$ M, the threshold concentration of chlorite needed for the formation of chlorine dioxide was 0.0024 M, which is very close to the 2:1 ratio obtained in reaction R1.

Acid Dependence. Acid concentrations influenced the induction period as well as the rate of formation and amount of chlorine dioxide formed after the induction period. The effect of acid varied depending on oxidant-to-reductant ratios as well as the range of acid concentrations used. In highly acidic conditions, $[H^+]_0 > 0.10$ M with $2 \leq R \leq 4$, acid concentrations reduced the induction period (see Figure 3a). This effect on the induction period is not as pronounced as that observed with chlorite (see Figures 2a,b). These acid concentrations did not affect the rapid rate of formation of chlorine dioxide at the end of the induction period. Higher acid concentrations, however, produced lower concentrations of chlorine dioxide (see, again, Figure 3a). This was unexpected since it is known that chlorine dioxide formation is from interactions among oxychlorine species which are universally accepted as acid-catalyzed. The depressed concentrations of chlorine dioxide are possible only if reactions in the reaction mixture that form chlorine dioxide are retarded by acid or if chlorine dioxide consumption reactions are acid catalyzed. Surprisingly, also, lower acid concentrations $0.005 \text{ M} < [H^+] < 0.015$ M, had no visible effect on the induction period (see Figures 3b and c). At lower ratios, $2 < R < 4$, there was no sharp and discernible induction period, but a swift and instant formation of chlorine dioxide. At higher ratios, $R \geq 10$, the reactions showed an invariant induction period irrespective of changes in acid (Figures 3a and b) and in PTU concentrations. Figure 3b shows a series of experiments undertaken at low acid concentrations showing the general increase in chlorine dioxide formed as acid is increased. However, between acid concentrations of 0.015 and 0.020 M, this trend is reversed (Figure 3c) and further increases in acid concentrations results in production of reduced amounts of chlorine dioxide. Separation of Figures 3b and c is to enable us to best display this reversal in trend.

The Chlorite−Phenylthiourea Ratio. There were two ways of altering oxidant-to-reductant ratio, *R*. One involves fixing the initial chlorite concentrations and varying $[PTU]_0$ (see Figure 4), and the other involves altering both $[ClO_2^-]_0$ and $[PTU]_0$ simultaneously (see Figure 5). In Figure 4, traces c, d, and e have $R < 2$; and so, ultimately, at t_∞, the final chlorine dioxide concentrations decayed to zero. The observed chlorine dioxide formation within the first 30 s of this reaction was only transient. As expected, higher PTU concentrations gave longer induction periods and faster rates of formation of chlorine dioxide. This is to be expected if the reactive species that control the formation of chlorine dioxide are derived from the oxidation of PTU or reduction of ClO_2^-. Figure 5 shows a wider range of ratios; $10 > R > 1.7$. Low ratios, e.g., traces a, b, and c in Figure 5, gave transient formation of chlorine dioxide, while higher ratios gave a monotonic increase in chlorine dioxide. Figure 5 can be regarded as an extension of the time scale shown in Figure 4.

Chlorine Dioxide Formation. Previous studies that involved chlorite oxidations have used the formation of chlorine dioxide as a means of following the reaction and evaluating kinetics

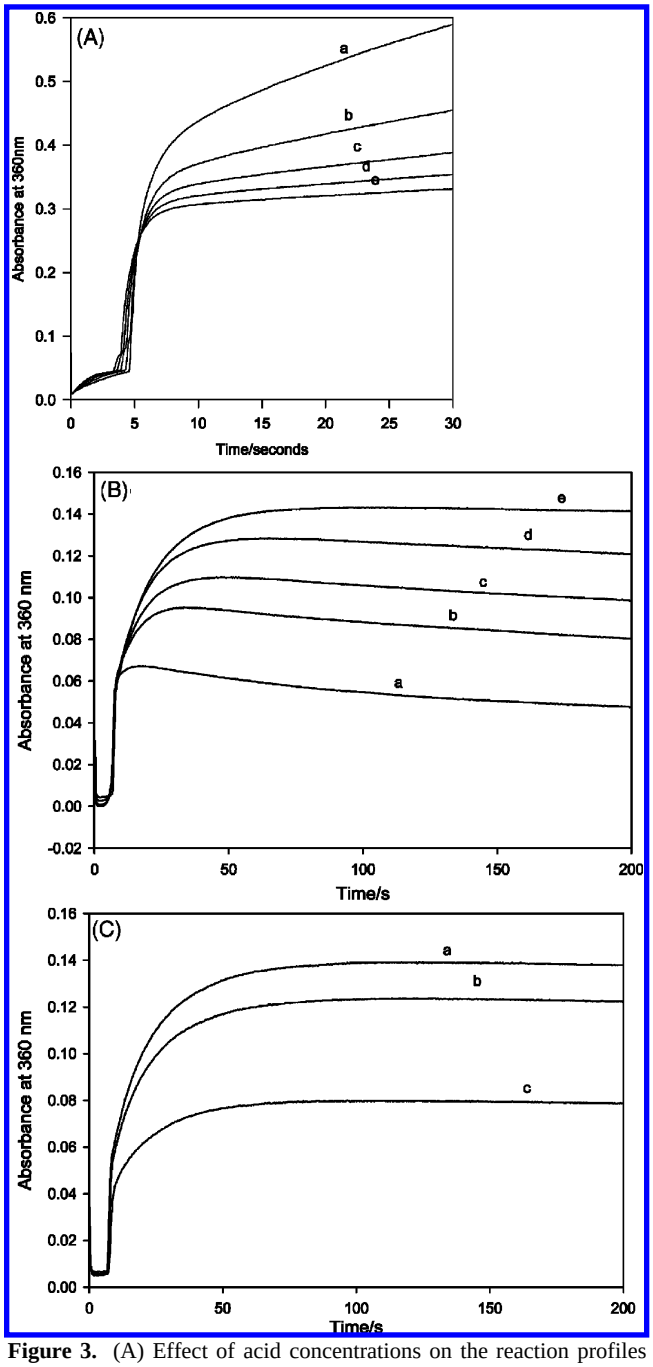

Figure 3. (A) Effect of acid concentrations on the reaction profiles with $[ClO_2^-]_0/[PTU]_0 = 4.00$. The observed induction period before formation of chlorine dioxide as well as the rate of formation of chlorine dioxide become insensitive to acid at high concentrations. $[PTU]_0 = 1.25 \times 10^{-3}$M, $[ClO_2^-]_0 = 5.0 \times 10^{-3}$M, $[H^+]_0 =$ (a) 0.1 M, (b) 0.2 M, (c) 0.3 M, (d) 0.4 M, and (e) 0.5 M. (B) The effect of acid undertaken at high $[ClO_2^-]_0/[PTU]_0$ ratio of 10.0. In this series of experiments, in low acid concentrations, acid catalyzes formation of chlorine dioxide, which is the exact opposite trend to the one shown in Figure 3A at high acid concentrations. The pH of the reaction medium in this series of experiments is above that of the pK_a of chlorous acid. $[PTU]_0 = 2.0 \times 10^{-4}$ M, $[ClO_2^-]_0 = 2.0 \times 10^{-3}$ M, $[H^+]_0 =$ (a) 0.0025 M, (b) 0.005 M, (c) 0.0075 M, (d) 0.01 M, (e) 0.015 M. (C) This figure shows the exact acid concentrations for reversal of the acid effect on chlorine dioxide formation. The figure shows that as pH of reaction medium goes below 1.7 (0.02 M acid), less and less chlorine dioxide is formed. $[PTU]_0 = 2.0 \times 10^{-4}$ M, $[ClO_2^-]_0 = 2.0 \times 10^{-3}$ M, $[H^+]_0 =$ (a) 0.02 M, (b) 0.025 M, (c) 0.05 M.

constants.[23] Chlorine dioxide is formed, in oxychlorine−organosulfur reaction systems, by an extraneous and purely oxyhalogen reaction that does not involve the substrate that is

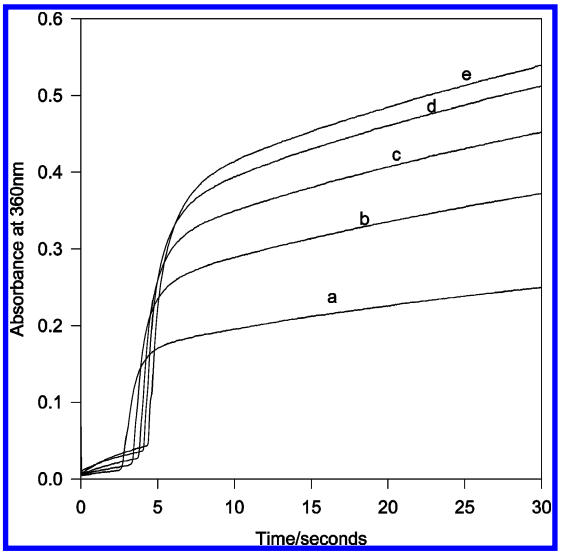

Figure 4. Effect of varying $PTU]_0$ on the formation of chlorine dioxide at fixed chlorite concentrations. Concentration of PTU is directly proportional to the amount of chlorine dioxide produced and to the induction period at fixed chlorite concentrations. $[ClO_2^-]_0 = 5.0 \times 10^{-3}$ M, $[H^+]_0 = 0.125$ M, $[PTU]_0 =$ (a) 2.5×10^{-4} M, (b) 5.0×10^{-4} M, (c) 7.5×10^{-4} M, (d) 1.0×10^{-3} M, and (e) 1.25×10^{-3} M.

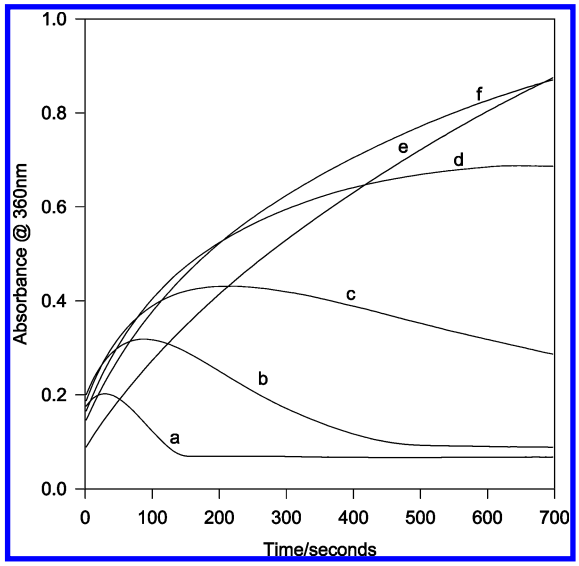

Figure 5. Effect of $[ClO_2^-]_0/[PTU]_0$ ratio on the absorbance traces at 360 nm. At high ratios of 4 and above, there is a monotonic formation of chlorine dioxide. At lower ratios, there is transient formation of chlorine dioxide. Trace (b) represents the exact stoichiometric ratio that does not produce chlorine dioxide at the end of the reaction but clearly shows transient chlorine dioxide formation. $[HClO_4]_0 = 0.125$ M, $[ClO_2^-]_0 = 2.5 \times 10^{-3}$ M. $[PTU]_0 =$ (a) 1.5×10^{-3} M, (b) 1.25×10^{-3} M, (c) 1.0×10^{-3} M, (d) 7.5×10^{-4} M, (e) 5.0×10^{-4} M, (f) 2.5×10^{-4} M.

being oxidized.[27] In nonradical processes, the first reactive oxyhalogen species formed in chlorite oxidations is hypochlorous acid, HOCl.[28,29] HOCl will then react very rapidly with remaining chlorite to produce chlorine dioxide:[27]

$$2ClO_2^- + HOCl + H^+ \rightarrow 2ClO_2(aq, yellow) + Cl^- + H_2O \quad (R5)$$

Three factors will determine whether chlorine dioxide is formed. (i) if the rate of reaction between the reducing substrate and chlorine dioxide is fast, then there will be no observation of chlorine dioxide until the reducing substrate and its oxidation intermediates have been completely oxidized. (ii) In large ratios, $R > 4$ (which is much higher than the required stoichiometry of $R = 2$), production of ClO_2 will overwhelm the small concentrations of substrate present such that there will be an immediate formation of ClO_2. Transient and complex ClO_2 formation can be obtained at low ratios, typically below 4. (iii) If rate of reaction of chlorine dioxide with the reducing substrate is slow, then oligooscillatory behavior will be obtained for reaction solutions with $R < 2$. A clear illustration of this can be seen in the data shown in Figure 5. Monotonic ClO_2 formation is obtained at ratios above 2.5 for acid concentrations of 0.125 M. This threshold ratio will change at different pH conditions. After long incubation times, all experiments with ratios below 2 will show no final chlorine dioxide accumulations (see stoichiometry R1 and Figure 5). The observed transient chlorine dioxide formation at these ratios clearly shows a delicate balance between reactions that form chlorine dioxide and those that consume it. The effect of chlorite concentrations (effectively, this is a variation in ratio, R) on the formation of chlorine dioxide is shown in the data in Figures 2a and 5. Traces with $R \leq 2$ will eventually have no chlorine dioxide at t_∞. For a fixed amount of acid concentrations, the rate of formation and transient amount of chlorine dioxide formed is directly proportional to the chlorite concentrations. This is to be expected if the formation of chlorine dioxide is mainly through reaction R5. The effect of acid on the reaction will be complex due to the fact that acid influences nearly all elementary reactions in this mixture. In some it is catalytic, and in some, inhibitory. Different acid effects will be observed at different pH conditions. The three main features of chlorine dioxide formation all change with acid: rate of formation of chlorine dioxide, maximum transient chlorine dioxide formed, and the rate of consumption of chlorine dioxide after attaining its peak. Ultimately, the overall global reaction dynamics will not show any specific dependence on acid. Figure 3a shows the high acid environment in which acid is inhibitory in the formation of chlorine dioxide. The ratio used in these data, $R = 4$, does not give an overwhelming excess of the oxidant, and thus the rate of consumption of ClO_2 by PTU and other reductants has to be factored into the determination of the overall reaction dynamics. Figure 3b, however, with $R = 10$, makes the observed chlorine dioxide formation a pure oxyhalogen reaction since most of the reducing organosulfur compound and its intermediates will have been completely consumed by the time chlorine dioxide is formed.

Oxidations by Chlorine Dioxide. Figures 6a,b, and c show the reaction of chlorine dioxide with PTU monitored at 360 nm. The reaction displays what appears to be a biphasic behavior, with, initially, sigmoidal autocatalytic kinetics, followed by normal decay (follow trace c in Figure 6a and all traces in Figures 6b and c). In excess of PTU, only the initial (autocatalytic) phase is observed (Figure 6a, traces a and b). Such sigmoidal decay kinetics have been consistently observed with respect to chlorine dioxide oxidations.[30] Figure 6b shows absorbance traces obtained in excess ClO_2. The autocatalytic phase lasts until a stoichiometric ratio of 4:5 is attained; i.e., 4 mol of ClO_2 to 5 mol of PTU. These data are summarized in Table 1. This ratio indicates that autocatalysis lasts until all the PTU has been oxidized to the sulfinic acid (see reaction stoichiometry R21). After this, a slow monotonic decay of chlorine dioxide is then observed up to the end of the reaction. A simple experiment was undertaken in which the synthesized sulfinic acid of PTU, phenylthiourea dioxide, (phenylaminoiminomethanesulfinic acid) was reacted directly with chlorine

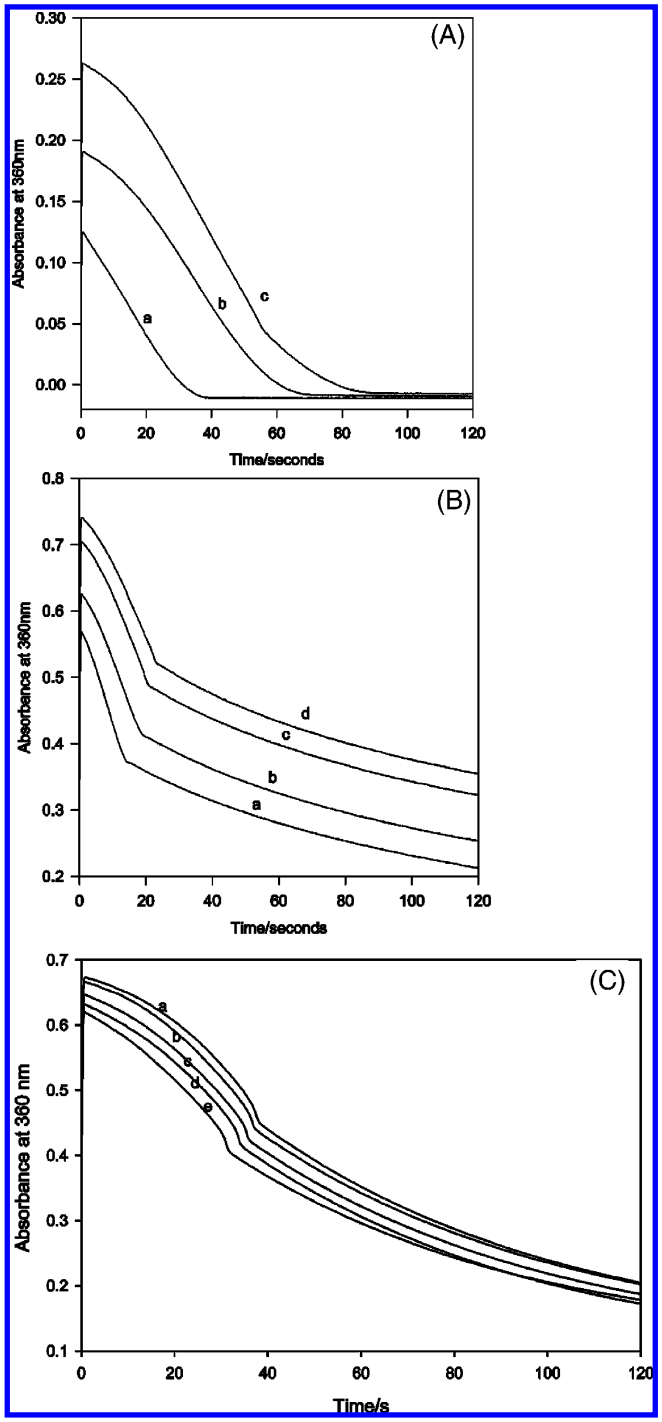

Figure 6. (A) Direct reaction of PTU and chlorine dioxide monitored at 360 nm with oxidant-to-reductant ratios below stoichiometric amounts. A single sigmoidal decay for the consumption of chlorine dioxide is observed for traces (a) and (b) in which the oxidation does not advance as far as the sulfinic acid. $[PTU]_0 = 2.5 \times 10^{-4}$ M, $[H^+]_0 = 0.125$ M, $[ClO_2]_0 =$ (a) 2.0×10^{-4} M, (b) 3.0×10^{-4} M, and (c) 4.0×10^{-4} M. (B) Chlorine dioxide oxidation at oxidant-to-reductant ratios; $[ClO_2]_0/[PTU]_0 > 2$. This shows two distinct steps of an initial sigmoidal decay followed by a standard decay. $[PTU]_0 = 2.5 \times 10^{-4}$ M, $[H^+]_0 = 0.125$ M, $[ClO_2]_0 =$ (a) 7×10^{-4} M, (b) $= 8 \times 10^{-4}$ M, (c) 9×10^{-4} M, and (d) $= 1 \times 10^{-3}$ M. (C) Observed effect of chlorite on the oxidation of PTU by chlorine dioxide. At micromolar quantities, chlorite accelerates the reaction and maintains two-stage kinetics. $[PTU]_0 = 2.5 \times 10^{-4}$ M, $[ClO_2]_0 = 6.76 \times 10^{-4}$ M, $[H^+]_0 = 0.125$ M, $[ClO_2^-]_0 =$ (a) 0, (b) 5×10^{-6} M, (c) 1.5×10^{-5} M, (d) 3.0×10^{-5} M, (e) 5.0×10^{-5} M.

dioxide. This experiment showed that the reaction of the sulfinic acid and chlorine dioxide was exceedingly slow, much slower than the reaction of chlorine dioxide with PTU. Previous reports on chlorine dioxide oxidations had suggested that the initial part of the reaction involves the formation of ClO_2^-, with subsequent oxidations being undertaken by chlorite.[20] Addition of chlorite in ClO_2 oxidations should show a catalytic effect. Data in Figure 6c indicate that this, indeed, is the case. Only micromolar quantities of chlorite were used in this series of experiments, and yet the effect is quite noticeable. The initial autocatalytic part of the reaction is the one that is immediately catalyzed with the rest of the reaction not catalyzed any further. This is evidence that chlorite is indeed the dominant pathway utilized by chlorine dioxide oxidations. The parallel nature of the absorbance traces after addition of chlorite also suggest that chlorite is not an autocatalytic species since its catalytic effect is linear and dependent solely on the amount of chlorite anions added.

TABLE 1: Analysis of Absorbance Data from Figure 6B[a]

$[ClO_2]_0$/M	$[PTU]_0$/M	$[ClO_2]_t$ at end of autocatalysis	$\Delta[ClO_2]/\Delta[PTU]$	expected $\Delta[ClO_2]/\Delta[PTU]$ for formation of sulfinic acid	deviation observed
0.0006	0.00025	0.000418	0.728	0.800	7.20%
0.000574	0.00025	0.000387	0.748	0.800	5.2%
0.000514	0.00025	0.000328	0.744	0.800	5.6%
0.000465	0.00025	0.000278	0.748	0.800	5.2%

[a] This table shows that the reaction slows down after a nearly quantitative formation of the sulfinic acid, indicating that the reaction between ClO_2(aq) and the sulfinic acid is very slow. This is also the position when chlorine dioxide formation commences (see Figure 10).

Data Collected at 249 nm. Figure 1 shows that PTU has a sharp and isolated peak in its UV spectrum at 249 nm. The products of its oxidation, phenylurea, as well as chlorine dioxide, also absorb at this wavelength, but with lower extinction coefficients. Data collected at this wavelength can deliver unambiguous initial rates of consumption of PTU at the beginning of the reaction before the reaction product starts to accumulate in the reaction medium. Figure 7a shows a typical series of runs performed at 249 nm. They show an initial rapid decrease in absorbance signal which quickly damps out to give way to a slower decrease in absorbance. This sequence would appear to be the opposite of that observed in Figures 6a,b, and c. The damping out of the absorbance decrease is due to the formation of an intermediate which is long-lived enough to be able to accumulate. If one compares comparable data from Figures 7a and 6b, one notices that the onset of damping in Figure 7a coincides with the end of the autocatalytic phase in Figure 6b. The very sharp and abrupt halt in absorbance decrease shown in Figure 7a is due to the final formation of the product which contributes substantially to the final absorbance observed. The data in Figure 7a give a linear dependence of the initial rate of PTU consumption with initial chlorite concentrations (Figure 7b). Induction period data (see Figure 2b) had also suggested a first order dependence of the reaction rate to chlorite concentrations. Direct oxidation of PTU by chlorine dioxide, monitored at 249 nm, gives traces that display autocatalysis (Figure 7c). This is in agreement with the data obtained in Figures 6a−c. Figure 8a shows the same types of absorbance traces as those shown in Figure 7a but with variable acid concentrations. Contrary to the data obtained at 360 nm with chlorine dioxide, the depletion kinetics of PTU are monotonic and less complex. Figures 8a and 8b show the effects of acid on the initial rate of consumption of PTU. Low acid concentrations display a saturation at about 0.02 M $HClO_4$ (Figure 8b). If the acid is further increased, a retardation is observed. Figure

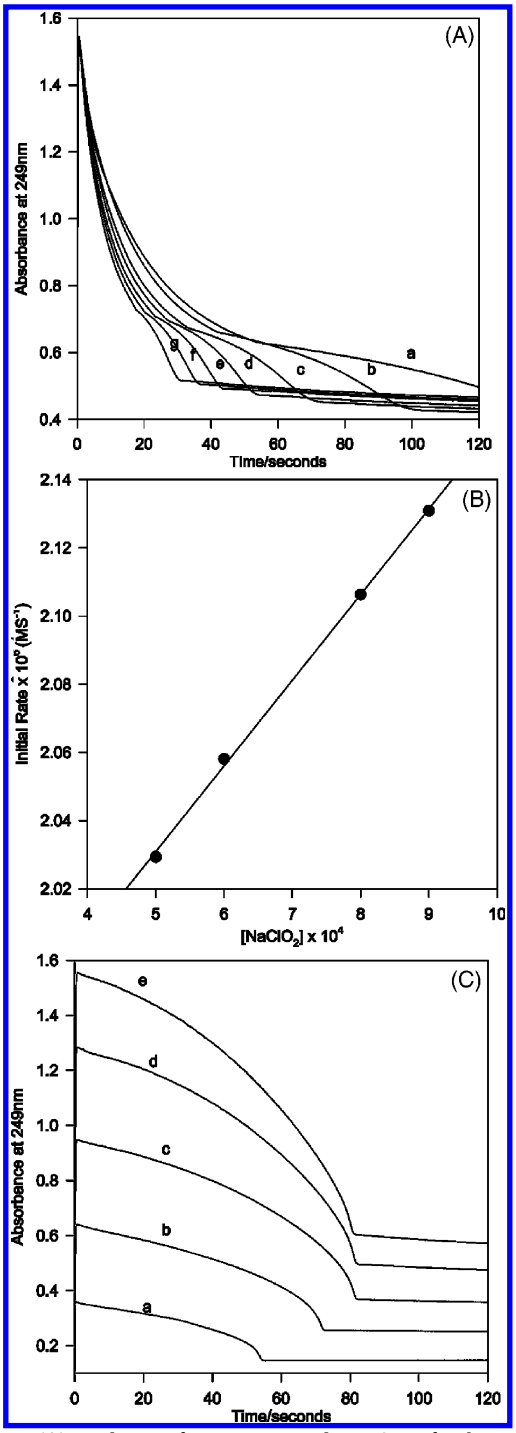

Figure 7. (A) Depletion of PTU monitored at 249 nm for the oxidation by chlorite. These data also display two-stage kinetics. The products of PTU oxidation, phenylurea, and chlorine dioxide give the residual absorbance that can be seen in the absorbance-time traces. $[PTU]_0 = 1.25 \times 10^{-4}$ M, $[HClO_4]_0 = 0.125$ M, $[ClO_2^-] =$ (a) 4.0×10^{-4} M, (b) 5.0×10^{-4} M, (c) 6.0×10^{-4} M, (d) 7.0×10^{-4} M, (e) 8.0×10^{-4} M, (f) 9.0×10^{-4} M, and (g) 1.0×10^{-3} M. (B) Relationship between initial rate of consumption of PTU and initial chlorite concentrations from the data shown in Figure 7A. There is a solid linear dependence. $[PTU]_0 = 1.25 \times 10^{-4}$ M, $[HClO_4]_0 = 0.125$ M. (C) Depletion of PTU in its oxidation by chlorine dioxide monitored at 249 nm. In high excess chlorine dioxide environments (ratios > 3), a single sigmoidal decay is observed for the consumption of PTU. This is in agreement with Figure 6A. $[ClO_2]_0 = 4.27 \times 10^{-4}$ M, $[H^+]_0 = 0.125$ M, $[PTU]_0 =$ (a) 2.5×10^{-5} M, (b) 5.0×10^{-5} M, (c) 7.5×10^{-5} M, (d) 1.0×10^{-4} M, and (e) 1.25×10^{-4} M.

8c summarizes the acid effect by combining a series of acid concentrations that range from 0.025 to 0.50 M. Very low acid concentrations show a sigmoidal autocatalytic decay of the peak at 249 nm (not shown in Figure 8c), and a gradual increase in acid will change the kinetics trace from this convex shape to a straight line zero order type kinetics (trace a) and finally to the standard concave decay kinetics curves that are observed in very high acid environments (traces d−f). The important aspect of Figure 8c to note is that the second phase of the reaction is much faster in low acid concentrations, while in high acid concentrations this intermediate species formed lingers much longer before forming products.

Chlorine Dioxide Oxidations Monitored at 249 nm. Figures 9a,b show the depletion kinetics of PTU with chlorine dioxide as the oxidant. Figure 9a shows the dominance of sigmoidal kinetics even in excess oxidant conditions, although the observed autocatalysis decreased with increase in oxidant concentrations. A high excess of oxidant, however, still did not afford pseudo-first order kinetics. In highly excessive oxidant concentrations, the depletion kinetics of PTU approached zero order. Figure 9b shows the effect of acid at low acid concentrations. Acid, at these conditions, $1.3 < pH < 2.7$, acid is very effective in inhibiting the reaction with respect to rate of consumption of PTU. If acid is increased further, past the concentrations shown in Figure 9b, its inhibition effect saturates.

Combining Data at 360 nm and at 249 nm. Figure 10 superimposes data collected at 249 nm and at 360 nm. This shows that chlorine dioxide formation commences at the start of the second phase of the reaction when monitored at 249 nm. This is an important experimental observation: whatever intermediate is formed or accumulated during the second phase of the reaction; it must be inert to (or reacts very slowly with) chlorine dioxide (hence its accumulation). This fact, combined with the experiment that showed a very slow reaction between chlorine dioxide and phenylthiourea sulfinic acid as well as data shown in Figure 6b (summarized in Table 1), indicate that this intermediate species is the sulfinic acid.

Mechanisms

Chlorite−PTU Reaction. We are assuming a nonradical pathway in which the initial stages of the reaction involve the formation of the reactive oxyhalogen species, HOCl:

$$ClO_2^- + PhN(H)CSNH_2 \rightarrow PhN{=}CS(OH)NH_2 + OCl^-;\ k_1 \quad \text{(R6)}$$

followed by

$$OCl^- + H^+ \equiv HOCl;\ K_{a2} \quad \text{(R7)}$$

$PhN{=}CS(OH)NH_2$ represents the unstable sulfenic acid which can either be oxidized further to a sulfinic acid, $PhN{=}CS(O_2H)NH_2$ (R8),[31] or can combine with another PTU molecule to form a stable dimer (R9).

$$ClO_2^- + PhN{=}CS(OH)NH_2 \rightarrow PhN{=}CS(O_2H)NH_2 + OCl^- \quad \text{(R8)}$$

$$PhN{=}CS(OH)NH_2 + PhN(H)CSNH_2 \rightarrow (PhN{=}C(NH_2)\text{-}S)_2 + H_2O \quad \text{(R9)}$$

The sulfenic acid can also disproportionate into the more stable PTU and the sulfinic acid:

$$2PhN{=}CS(OH)NH_2 \rightleftharpoons PhN{=}CS(O_2H)NH_2 + PhN(H)CSNH_2 \quad \text{(R10)}$$

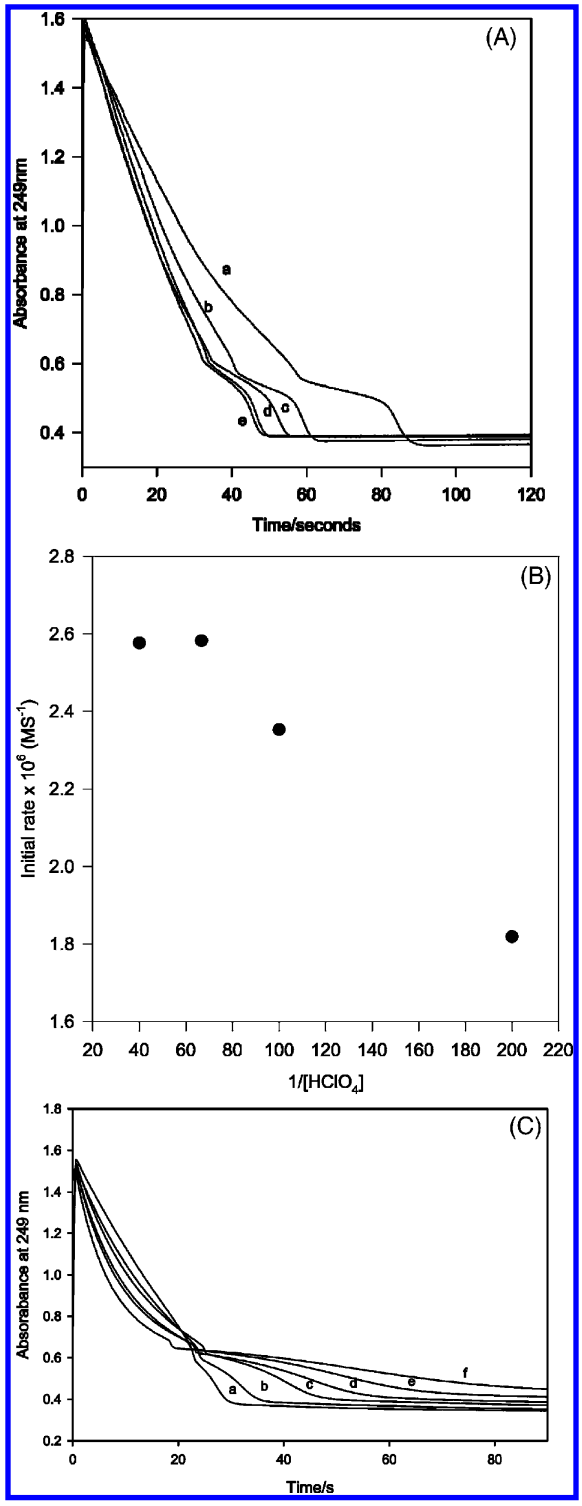

Figure 8. (A) Absorbance traces at 249 nm showing the effect of acid on the rate of consumption of PTU at low acid concentrations. Acid catalyzes the first stage of the reaction but appears to retard the second stage. $[PTU]_0 = 1.25 \times 10^{-4}$ M, $[ClO_2^-]_0 = 5.0 \times 10^{-4}$ M, $[HClO_4]_0$ = (a) 0.005 M, (b) 0.010 M, (c) 0.015 M, (d) 0.020 M, (e) 0.025 M. (B) Initial rate plots for low acid concentrations. A maximum rate of consumption is attained at approximately pH 2.00. Higher acid concentrations show a retardation of the rate of consumption of PTU. (c) A combination of high and low acid concentrations and their effects on the ClO_2^-−PTU reaction. High acid concentrations involve oxidation by $HClO_2$ and give a fast first step and slower second step (trace f), while low acid concentrations involve oxidation by both $HClO_2$ and ClO_2^-, followed by a much faster second step (trace a). $[PTU]_0 = 1.25 \times 10^{-4}$ M, $[ClO_2^-]_0 = 7.0 \times 10^{-4}$ M, $[HClO_4]_0$ = (a) 0.025M, (b) 0.05 M, (c) 0.1 M, (d) 0.15 M, (e) 0.20 M, (f) 0.50 M.

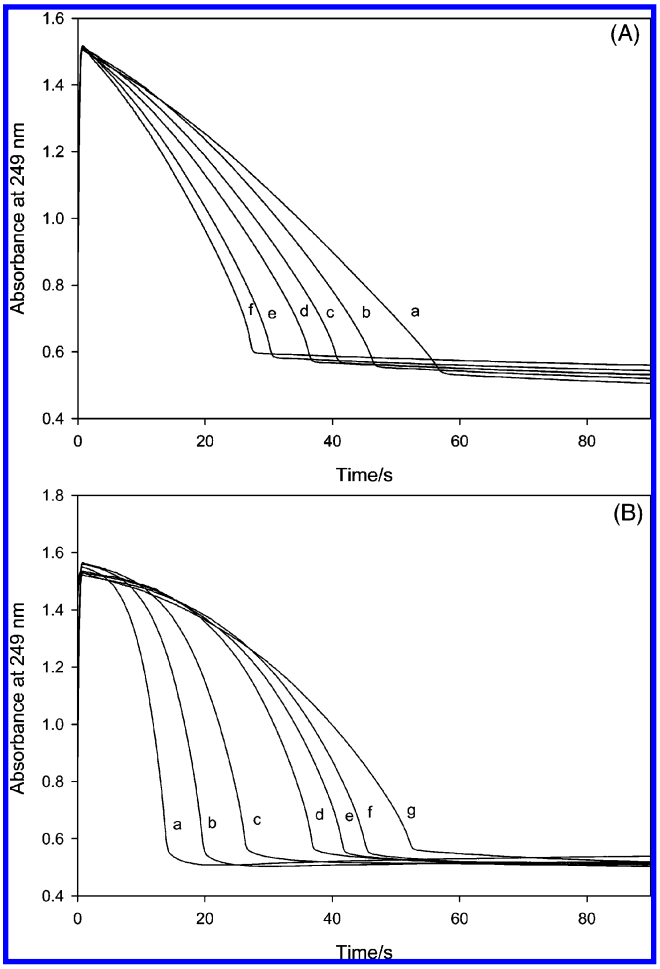

Figure 9. (A) Chlorine dioxide oxidation: In stoichiometric excess chlorine dioxide, a single sigmoidal decay curve for the consumption of PTU at 249 nm is observed. $[PTU]_0 = 1.25 \times 10^{-4}$ M, $[HClO_4]_0 = 0.125$ M. $[ClO_2]_0$ = (a) 1.69×10^{-4} M, (b) 3.38×10^{-4} M, (c) 4.23×10^{-4} M, (d) 5.07×10^{-4} M, (e) 6.76×10^{-4} M, (f) 8.45×10^{-4} M. (B) Low acid variation in the oxidation of PTU by chlorine dioxide. In this case, low acid concentrations are inhibitory. All traces show sigmoidal decay kinetics. $[PTU]_0 = 1.25 \times 10^{-4}$ M; $[ClO_2]_0$ = (a) 3.38×10^{-4} M; $[H^+]_0$ = (a) 0.0025 M, (b) 0.005 M, (c) 0.01 M, (d) 0.015 M, (e) 0.020 M; (f) 0.025 M, (g) 0.05 M.

Literature has several reports of formation of thiosulfinates from sulfenic acids in the absence of further oxidant.[32] After the initiation reaction R6, the sulfenic acid can only react through reactions R8−R10. There seems to be no other fate for the sulfenic acid. In excess oxidant, the favored pathway is R8. In limited amounts of oxidant (e.g., 1:1 mixture ratios of PTU with an equivalent of a two-electron oxidant), quantitative dimer formation can be obtained as in reaction R9. A bulky dimer, of the type formed in reaction R9, however, due to its expected low solubility should precipitate from solution. No precipitate was observed in our experimental observations, thus precluding reaction R9 as a major route in this mechanism. We expect, then, that upon depletion of oxidant, reactions of R10-type will dominate such that the favored stable forms of the sulfur compound are formed: PTU itself, the sulfinic acid, or sulfate. In our proposed mechanism, the rate-determining step in the oxidation of PTU by chlorite is reaction R6. Reaction R6, as well as any other reactions that involve the reduction of a chlorine center coupled to the oxidation of a sulfur center, will be considered irreversible in this mechanism. Reaction R7 is a rapid protolytic step such that R6 and R7 can be combined as one reaction even though we recognize that R11 is not a

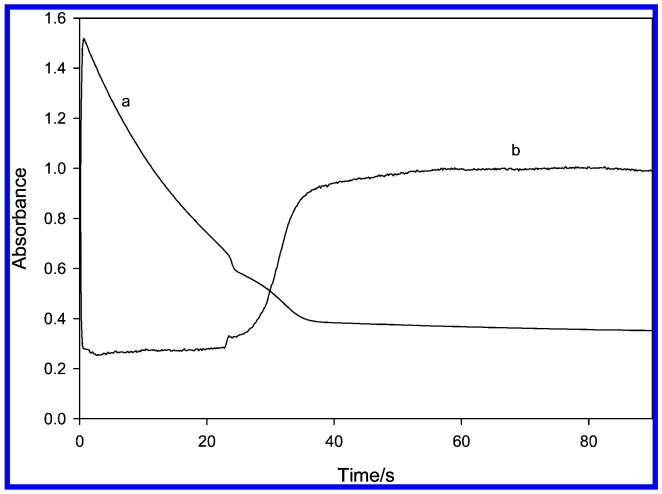

Figure 10. Superimposition of traces at 249 and 360 nm. The trace at 360 nm (trace b) had to be amplified 40x to be on the same scale with the trace at 249 nm. Chlorine dioxide formation commences *exactly* at the end of the first stage of the reaction. $[PTU]_0 = 1.25 \times 10^{-4}$ M; $[ClO_2^-]_0 = 7.0 \times 10^{-4}$ M; $[H^+]_0 = 0.050$ M.

termolecular process:

$$ClO_2^- + PhN(H)CSNH_2 + H^+ \rightarrow PhN{=}CS(OH)NH_2 + HOCl \quad (R11)$$

R11 is an initial electrophilic attack on PTU followed by protonation and elimination of HOCl. Our acid dependence data can be explained by the effectiveness of the direct reaction of chlorous acid with PTU:

$$HClO_2 + PhN(H)CSNH_2 \rightarrow PhN{=}CS(OH)NH_2 + HOCl;\ k_2 \quad (R12)$$

The complex acid dependence data obtained can be explained on the basis of protonation equilibria for both chlorous acid and PTU:

$$ClO_2^- + H^+ \rightleftharpoons HClO_2;\ K_{a1}^{-1} \quad (R13)$$

$$PhN(H)CSNH_2 + H^+ \rightleftharpoons [PhN(H)CS(H)NH_2]^+;\ K_b \quad (R14)$$

In reaction R13, K_{a1} is the acid dissociation constant for chlorous acid. Our kinetics data have suggested that, initially, the rate of depletion of PTU is first order in both PTU and chlorite with a complex order with respect to acid. If it is assumed that $HClO_2$ is relatively inert (R12 route negligible), then the rate of reaction can be derived in terms of chlorite and PTU. The total Cl(III) species in solution are partitioned between ClO_2^- and $HClO_2$ according to the following mass balance equation:

$$[Cl(III)]_T = [ClO_2^-] + [HClO_2] \quad (1)$$

From the following relationship:

$$[HClO_2] = \frac{[ClO_2][H^+]}{K_{a1}} \quad (2)$$

chlorite concentrations can be written in terms of the total chlorine(III) species:

$$[ClO_2^-] = \frac{K_{a1}[Cl(III)]_T}{K_{a1} + [H^+]} \quad (3)$$

The derived rate of reaction with R6 as the single and rate-determining step will be given by eq 4:

$$\text{Rate} = -\frac{d[PTU]}{dt} = k_1\frac{[PTU][Cl(III)]_T[H^+]}{(1 + K_{a1}^{-1}[H^+])} \quad (4)$$

Our experimental data do not support eq 4 for all the pH ranges studied. Equation 4 suggests retardation when $[H^+] \gg K_{a1}$, as the term with acid concentration in the denominator will dominate. The equation also suggests that the inhibitory effect of acid will diminish at low acid concentrations, pH > pK_{a1}, but does not support acid catalysis in any pH range. The experimentally observed acid catalysis effect may have its genesis from the oxychlorine reactions that produce the reactive species. Our data would suggest, then, that reaction R12, in which the protonated chlorous acid reacts directly with PTU, contributes significantly to the overall reaction rate observed, and is, in fact, the dominant pathway. K_{a1} has been reported[33] to be approximately 0.0191 M^{-1}. One would thus expect saturation in acid effect with no further retardation in conditions of pH lower than 2.0, which represents the approximate pK_a range of chlorous acid. The rate of reaction can now be derived using both reactions R6 and R12 to obtain the following rate law:

$$\text{Rate} = -\frac{d[PTU]}{dt} = \frac{[Cl(III)]_T[PTU]_0}{K_{a1} + [H^+]}[k_1K_{a1} + k_2[H^+]] \quad (5)$$

Experimental Evaluation of Kinetics Parameters k_1 and k_2. The important kinetics parameters in this reaction system are the rate constants for the reaction between PTU and ClO_2^- (k_1), $HClO_2$ (k_2), and with ClO_2(aq). The reaction's acid dependence, on its own, was too complex to be utilized for the evaluation of k_1 and k_2. Two complementary experimental techniques had to be used for evaluating $k_1$and k_2. The values obtained in these two methods could then be checked against each other. Equation 5 was utilized for this evaluation by running a series of experiments at fixed acid concentrations and collecting initial rates of consumption of PTU at 249 nm. By running a series of experiments at varying combinations of $[PTU]_0$ and $[ClO_2^-]_0$, a plot could be made of initial rate of reaction vs the product of $[PTU]_0$ and $[Cl(III)]_T$. This plot was preferred over others (e.g., a $[PTU]_0$ dependence plot or $[ClO_2^-]_0$ dependence plot) because it gave the origin as a firm data point. In our statistical and graphical analysis, we could weight the origin of such a plot and thus greatly reduce experimentally generated errors. The slope of the linear part of this plot gave the value of the term in the brackets of eq 5; but not individual values of k_1 and k_2. Next, using as a rough estimate Figure 8c, trace c (for example) was utilized to evaluate k_2 in the limit of high acid where only the second term in eq 5 was relevant. This value was brought back into eq 5 as the initial value to then fit the initial rate data and evaluate unambiguous values of k_1 and k_2, with their relevant error ranges. The second complementary set of experiments involved the use of low acid concentrations in which both $HClO_2$ and ClO_2^- species were relevant. Three acid concentrations were used: 0.001, 0.003, and 0.005 M. For each of these acid concentrations, six experiments were performed at specific chlorite concentrations and initial rates were derived and recorded. Six plots of initial rate vs acid were generated and k_1 (intercept) and k_2 (slope) values were evaluated. These values were then refined by the use of the more accurate data set from the first series of experiments. The final values adopted were from this (first) set. This very extensive analysis gave k_1

$= 31.5 \pm 2.3\ M^{-1}\ s^{-1}$ and $k_2 = 114 \pm 7.0\ M^{-1}\ s^{-1}$. The fact that $k_2 > k_1$ was to be expected since an electrophilic attack by chlorite on the nucleophilic sulfur atom of PTU will not be as facile as that by $HClO_2$. The fact that acid was catalytic at low acid concentrations establishes this fact.

Equation 5 supports a saturation of the initial rate as acid is further increased past the pK_a of chlorous acid. Our experimental observations show a retardation of the rate as acid concentrations are increased past 0.10 M. To accommodate this retardation, eq 5 has to be modified for these high acid environments. Under these conditions, the Cl(III) species will exist predominantly as $HClO_2$ with negligible amounts of unprotonated chlorite available. Any variations in rate can no longer be derived solely from the oxychlorine species. The protonation of thiocarbonyl compounds, like PTU, is well-known (reaction R14).[34] The nucleophilic sulfur center is easily protonated at low pH conditions. One would then expect substantial protonation of PTU at the conditions of $[H^+] > 0.10$ M. We can assume that the protonated PTU species is inert and combine pathways R6, R12, and the retarding effect of protonation of PTU, R14, to give an overall rate of reaction:

$$\text{Rate} = -\frac{d[\text{PTU}]}{dt} = \frac{[\text{Cl(III)}]_T[\text{PTU}]_0}{(1 + K_b[H^+])(K_{a1} + [H^+])}[k_1K_{a1} + k_2[H^+]] \quad (6)$$

Equation 6 assumes negligible reaction between chlorous acid and protonated phenylthiourea. A more complete rate law would include the reaction between chlorite anion and the protonated phenylthiourea, but this pathway would be negligible in this scheme because high pH conditions would increase $[ClO_2^-]$ while decreasing the protonated thiol concentration, while low pH conditions would decrease $[ClO_2^-]$ while increasing the protonated thiocarbamide (PTU). Equation 6 would deliver the observed complex acid dependence behavior of initial acid catalysis followed by saturation and then retardation. In highly acidic conditions, eq 6 can be utilized with very little loss in precision, without the first term in the square bracket and the second bracketed term in the denominator which involve reaction by chlorite. This simplification of eq 6 was used in the evaluation of k_2 for data shown in Figure 8c where it was assumed $[\text{Cl(III)}]_T \approx [HClO_2]$.

The observed variations of rate with acid concentrations depend on the relative magnitudes of k_1 and k_2. Our experimental observations indicate acid catalysis up to approximately pH 2.00 followed by a saturation and retardation as acid concentrations are increased past this point. This would indicate a dominance of k_2 with the further retardation upon saturation of $[HClO_2]$ being effected by the $1 + K_b[H^+]$ term, which represents protonation of the thiocarbonyl group. Equations 5 and 6 predict this trend.

Formation of Chlorine Dioxide. Chlorine dioxide is formed by the one-electron oxidation of chlorite. Two possible oxidizing species in this reaction medium are hypochlorous acid (see reaction R5)[26,27] and molecular chlorine.[35] The standard disproportionation reactions that can produce chlorine dioxide are too slow to be effective on this time scale. The kinetics of the hydrolysis of chlorine have been studied by temperature-jump spectrophotometry, and the kinetics parameters are well known:[36]

$$Cl_2 + H_2O \rightleftharpoons HOCl + H^+ + Cl^- \quad (R15)$$

This is a rapid equilibrium, and so the oxidation of chlorite by HOCl (reaction R5) or by Cl_2 (reaction R16) should be kinetically indistinguishable.[37]

$$2ClO_2^- + Cl_2 \rightarrow 2ClO_2(aq) + 2Cl^- \quad (R16)$$

The mechanism of reaction R16 was studied by Nicoson and Margerum[38] and proceeds through some intermediate that involves an adduct of $ClO_2 \cdot Cl_2^-$, which can then eliminate a Cl^- ion after the transfer of a Cl^+ atom to ClO_2^-. The mechanism of the oxidation of chlorite by HOCl is also well known. Taube and Dodgen,[37] using isotopic labeling, have concluded that this oxidation proceeds through the asymmetric intermediate Cl_2O_2:[26,35,39]

$$ClO_2^- + HOCl + H^+ \rightleftharpoons Cl_2O_2 + H_2O \quad (R17)$$

Further reaction of the intermediate will yield ClO_2:

$$ClO_2^- + Cl_2O_2 \rightarrow 2ClO_2 + Cl^- \quad (R18)$$

Both R17 and R18 are not elementary single steps although the kinetics of these reactions can be derived from their molecularities.

It does appear that the rate of formation of HOCl from the reduction of ClO_2^- will determine the rate of formation of ClO_2. Composite reaction R11 (R6 + R7) is the only source of HOCl at the beginning of the reaction. As the reaction proceeds, the reaction of chlorite with sulfenic acid (produced in reaction R11) and other sulfur oxo-acids that are not oxidatively saturated will also yield HOCl.

Consumption of Chlorine Dioxide. Figure 5 shows that there is a delicate balance between the reactions that form chlorine dioxide and those that consume it. After eliminating R16, we can approximate that the sole reaction responsible for the formation of chlorine dioxide is reaction R5. Chlorine dioxide can be consumed by any of the reducing sulfur species in solution, but, due to its radical nature (unpaired electron), the most significant route is its direct reaction with PTU. Our kinetics data suggest first-order dependence in PTU and chlorine dioxide. The sigmoidal decay kinetics of chlorine dioxide oxidations (Figures 6a−c) suggest that the initial stages of the reaction involve the formation of the reactive species which then carries the bulk of the oxidation. This appears, in highly acidic conditions, to be $HClO_2$, which will ultimately produce HOCl. The radical chlorine center in chlorine dioxide is electron deficient with a strong formal positive charge, while the sulfur center in PTU is electron rich. An equilibrium is set up between chlorine dioxide and PTU with the formation of a loose adduct held together by a weak coordinate bond between the chlorine and sulfur centers:[20,40,41]

$$ClO_2 + S{=}C(NH_2)N(H)Ph \rightleftharpoons [O_2Cl\text{--}S{=}C(NH_2)N(H)Ph] \quad (R19)$$

This adduct can either return to the original reactants or react further with another chlorine dioxide molecule to form chlorous acid and the sulfenic acid after a hydrolysis:

$$[O_2Cl\text{--}S{=}C(NH_2)N(H)Ph] + ClO_2(aq) \rightarrow PhN{=}CS(OH)NH_2 + 2HClO_2 \quad (R20)$$

The rate-determining step is the formation of the adduct with R20 being relatively facile, irreversible, and entropy-driven. The irreversibility of R20 is supported by the reaction's inhibition by acid (see Figure 9b). Acid inhibition also proves that R19 is

the rate-determining step since protonation of PTU would inhibit formation of the adduct by forming a poorer nucleophile, $[PhN(H)CS(H)NH_2]^+$. If the protonated PTU is inert, then the rate of oxidation of PTU by chlorine dioxide will be given by:

$$-\frac{d[PTU]}{dt} = \frac{k_3[PTU][ClO_2]}{1 + K_b[H^+]} \quad (7)$$

In the limit of low acid concentrations, k_3 was evaluated from data of the type shown in Figures 6 and 9. The value obtained of $k_3 = 74 \pm 22\ M^{-1}\ s^{-1}$ was not very reliable due to uncertainties brought about by the sigmoidal decay-type kinetics as well as the uncertainty in the estimation of K_b.

Nonlinear Consumption and Formation of Chlorine Dioxide. Data in Figures 6a,b, and c display biphasic kinetics with an initially sigmoidal consumption of chlorine dioxide followed by a slower monotonic decay. While autocatalysis in chlorine dioxide formation has been rationalized through the formation of HOCl, this alone cannot explain the biphasic kinetics. Table 1 shows an analysis of the data in Figure 6b. The changeover from rapid autocatalytic kinetics occurred after the almost quantitative formation of the sulfinic acid of PTU:

$$4ClO_2(aq) + 5PhN(H)CSNH_2 + 2H_2O \rightarrow 5PhN{=}CS(O_2H)NH_2 + 4Cl^- + 4H^+ \quad (R21)$$

This suggests that chlorine dioxide is inert to phenylthiourea sulfinic acid or that this reaction is very slow. This was also proved by the observation that chlorine dioxide reacts very slowly with phenylthiourea sulfinic acid (refer to the Experimental Section for the preparation of phenylthiourea sulfinic acid) to the point of almost being inert. The accuracy of Figure 6b is derived from the fact that these experimental observations are being performed at 360 nm. Since neither PTU nor phenylurea absorb at 360 nm, our experiment can follow the consumption of chlorine dioxide almost exactly. The formation of the phenylthiourea sulfinic acid at the transition between sigmoidal kinetics and a normal decay is thus not in dispute. Figure 10 also confirms our assertion: chlorine dioxide is formed as soon as the sulfinic acid is formed. The observed rapid formation of ClO_2 in Figure 4 can also be explained similarly: The final observed rate of formation of ClO_2 is from a combination of the reactions that form ClO_2 (reaction R5), and those that consume it (reactions of type R19 + R20). Formation of the sulfinic acid, however, decreases the rate of consumption of $ClO_2(aq)$, and hence the observed sudden increase in the formation of $ClO_2(aq)$. An examination of Figure 10 confirms this analysis. The formation of the sulfinic acid, which is (relatively) inert to ClO_2 leaves reactions that form ClO_2 dominant over those that consume it, and hence the instant formation of ClO_2 upon commencement of the second phase of the reaction. Consumption of the sulfinic acid will then proceed predominantly through oxidation by $HClO_2$ and HOCl and very insignificantly by ClO_2. Chlorine dioxide's selective inertness is well known. In a previous submission from our laboratories, it was noted that the reaction of chlorite and formaldehyde delivered almost quantitative formation of chlorine dioxide based on stoichiometry R2 due to the inertness of chlorine dioxide to formaldehyde and formic acid.[42]

Formation of Phenylurea. Further oxidation of the phenylthiourea dioxide (intermediate species) will yield the sulfonic acid which can further be oxidized to yield phenylurea:

$$PhN{=}CS(O_2H)NH_2 + HOCl \rightarrow PhN{=}CS(O_3H)NH_2 + H^+ + Cl^- \quad (R22)$$

$$PhN{=}CS(O_3H)NH_2 + HOCl + H_2O \rightarrow PhN(H)CONH_2 + SO_4^{2-} + 3H^+ + Cl^- \quad (R23)$$

The accumulation of the sulfinic acid as an intermediate indicates that reactions R22 and R23 must be slower than R6, R8, and R12. Work by Makarov et al.[43] and Otoikhian et al.[44] proved that the oxidation of sulfinic and sulfonic acids predominantly goes through the initial cleavage of the C−S bond to give sulfoxylate anion and bisulfite respectively:

$$PhN{=}CS(O_2H)NH_2 + H_2O \rightarrow PhN(H)CONH_2 + HSO_2^- + H^+ \quad (R24)$$

$$PhN{=}CS(O_3H)NH_2 + H_2O \rightarrow PhN(H)CONH_2 + HSO_3^- + H^+ \quad (R25)$$

Further oxidation of the sulfur leaving groups should be rapid and nearly diffusion-controlled. These sulfur oxo-acids exist in the form of resonance-stabilized zwitterions that are much more stable in acid than in base.[43,45] This explains why the sulfinic acid intermediate is slower in reacting to form products in high acids but quickly gives products in low acid (see Figure 8c). The cleavage of the C−S bond in sulfinic and sulfonic acids in low acid environments is the basis for guanidylation.[46]

Overall Reaction Network. The chlorite−PTU and chlorine dioxide−PTU reactions can both be comprehensively explained by a single reaction network of 29 reactions which are shown in Table 2. Using relevant assumptions, these reactions can be severely truncated to only a few for high acid concentrations where chlorite oxidations are deleted in favor of those by chlorous acid. The direct reaction between chlorine dioxide and PTU can be derived by utilizing relevant reactions in Table 2 and deleting the rest.

The tabulated mechanism is divided into five distinct sections. Reactions M1−M3 represent the rapid protolytic reactions that are responsible for the observed complex acid dependence. Reaction M3 is relevant at much higher acid concentrations than M1 and M2. Reactions M4−M11 are reactions that involve oxidations by ClO_2^- and $HClO_2$. The whole reaction scheme is controlled by reactions M4 and M5 which represent the rate-determining steps. The set of reactions M12−M15 are the autocatalytic steps which also include formation of chlorine dioxide. M13 is the only reaction through which chlorine dioxide is formed throughout the whole mechanism, and in conditions of excess oxidant, its rate of formation will be dependent upon rate of formation of HOCl from the reduction of Cl(III) species. Reactions M16 − M19 represent the dominant oxidation pathway. The autocatalytic production of ClO_2 transfers the bulk of oxidation to HOCl, even though, at the beginning of the reaction, before the build-up of HOCl concentrations, the major oxidation pathway would have been the series of reactions M4−M11. Reactions M20−M23 involve oxidation by ClO_2. From the basis of our experimental observations, no reactions have been included that involve oxidation of the sulfinic and sulfonic acids by ClO_2. The set of four reactions, M24−M27 represent the hydrolysis of the sulfinic and sulfonic acids. While recent experimental data indicate that these oxo-acids are more stable in acidic environments,[43,45] this mechanism could not handle stabilization by acid. Further mechanistic studies need to be

TABLE 2: Chlorite−Chlorine Dioxide−Phenylthiourea Reaction Network[a]

number	reaction	k_f; k_r
M1	$ClO_2^- + H^+ \rightleftharpoons HClO_2$	1×10^9; 1.91×10^7
M2	$OCl^- + H^+ \rightleftharpoons HOCl$	1×10^9; 3.24×10^1
M3	$PhN(H)CSNH_2 + H^+ \rightleftharpoons [PhN(H)CS(H)NH_2]^+$	1×10^9; 1.12×10^6
M4	$ClO_2^- + PhN(H)CSNH_2 \rightarrow PhN{=}CS(OH)NH_2 + OCl^-$	32
M5	$HClO_2 + PhN(H)CSNH_2 \rightarrow PhN{=}CS(OH)NH_2 + HOCl$	115
M6	$ClO_2^- + PhN{=}CS(OH)NH_2 \rightarrow PhN{=}CS(O_2H)NH_2 + OCl^-$	5×10^3
M7	$ClO_2^- + PhN{=}CS(O_2H)NH_2 \rightarrow PhN{=}CS(O_3H)NH_2 + OCl^-$	95
M8	$ClO_2^- + PhN{=}CS(O_3H)NH_2 \rightarrow PhN(H)CONH_2 + SO_4^{2-} + Cl^- + 2H^+$	15
M9	$HClO_2 + PhN{=}CS(OH)NH_2 \rightarrow PhN{=}CS(O_2H)NH_2 + HOCl$	1×10^3
M10	$HClO_2 + PhN{=}CS(O_2H)NH_2 \rightarrow PhN{=}CS(O_3H)NH_2 + HOCl$	45
M11	$HClO_2 + PhN{=}CS(O_3H)NH_2 \rightarrow PhN(H)CONH_2 + SO_4^{2-} + Cl^- + 3H^+$	12
M12	$ClO_2^- + HOCl + H^+ \rightleftharpoons Cl_2O_2 + H_2O$	1.01×10^6; 0.1
M13	$Cl_2O_2 + ClO_2^- \rightleftharpoons 2ClO_2 + Cl^-$	1.5×10^3; 5.5×10^{-6}
M14	$Cl_2O_2 + PhN(H)CSNH_2 + H_2O \rightarrow PhN{=}CS(OH)NH_2 + 2HOCl$	2×10^3
M15	$Cl_2O_2 + PhN{=}CS(OH)NH_2 + H_2O \rightarrow PhN{=}CS(O_2H)NH_2 + 2HOCl$	1×10^3
M16	$HOCl + PhN(H)CSNH_2 \rightarrow PhN{=}CS(OH)NH_2 + H^+ + Cl^-$	5×10^3
M17	$HOCl + PhN{=}CS(OH)NH_2 \rightarrow PhN{=}CS(O_2H)NH_2 + H^+ + Cl^-$	2×10^3
M18	$HOCl + PhN{=}CS(O_2H)NH_2 \rightarrow PhN{=}CS(O_3H)NH_2 + H^+ + Cl^-$	100
M19	$HOCl + PhN{=}CS(O_3H)NH_2 \rightarrow PhN(H)CONH_2 + SO_4^{2-} + H^+ + Cl^-$	50
M20	$ClO_2 + S{=}C(NH_2)N(H)Ph \rightleftharpoons [O_2Cl{-}S{=}C(NH_2)N(H)Ph]$	74
M21	$[O_2Cl{-}S{=}C(NH_2)N(H)Ph] + ClO_2(aq) \rightarrow PhN{=}CS(OH)NH_2 + 2HClO_2$	1×10^3
M22	$ClO_2 + HOS{-}C(NH_2){=}NPh \rightleftharpoons [O_2Cl{-}(HO)S{-}C(NH_2){=}NPh$	50
M23	$[O_2Cl{-}(HO)S{-}C(NH_2){=}NPh \rightarrow PhN{=}CS(O_2H)NH_2 + 2HClO_2$	1×10^3
M24	$PhN{=}CS(O_2H)NH_2 + H_2O \rightarrow PhN(H)CONH_2 + HSO_2^- + H^+$	500
M25	$PhN{=}CS(O_3H)NH_2 + H_2O \rightarrow PhN(H)CONH_2 + HSO_3^- + H^+$	50
M26	$HSO_2^- + HOCl \rightarrow HSO_3^- + H^+ + Cl^-$	5×10^4
M27	$HSO_3^- + HOCl \rightarrow SO_4^{2-} + 2H^+ + Cl^-$	1×10^4
M28	$2ClO_2 + HSO_2^- + H_2O \rightarrow HSO_3^- + 2HClO_2$	4×10^6
M29	$2ClO_2 + HSO_3^- \rightarrow SO_4^{2-} + H^+ + 2HClO_2$	5×10^5

[a] Legend: $PhN{=}CS(OH)NH_2$, phenylthiourea sulfenic acid; $PhN{=}CS(O_2H)NH_2$, phenylthiourea sulfinic acid; $PhN{=}CS(O_3H)NH_2$, phenylthiourea sulfonic acid. Rate constants: forward and reverse rate constants (column 3) separated by a semicolon. Note: Reactions M8, M11, and M19 all require a molecule of solvent water for material balance. Units of rate constants derived from the reaction's molecularity except where water was involved, and also in M28 and M29 which are composites of two consecutive steps and considered bimolecular.

performed before a rate law for the decomposition of these oxoacids can be derived.

Choice and Establishment of Rate Constants. The first three reactions, being rapid and protolytic could be assigned any rate constants as long as they were fast enough so as not to be rate-determining and not violate the pK_a's of $HClO_2$ and HOCl as well as the pK_b pf the thiocarbamide. Since pK_a of chlorous acid[26,47] is 1.72; the forward and reverse rate constants utilized had to satisfy $K_a = 0.0191$. Literature reports pK_a of HOCl[26,33] as 7.49, and so this was also utilized in the same manner as for $HClO_2$. K_b for the thiocarbamide was difficult to evaluate, but a value of 8.9×10^2 M^{-1} was derived for a similar thiocarbamide: guanylthiourea.[34] However, protonation of PTU was only relevant in very high acid environments, while most of our work was performed in the intermediate acid concentration ranges where K_b was not relevant. In fact, for most of our simulations, this reaction was shut down with no loss of accuracy.

Rate constants for M4 and M5 were derived from this study. M6 and M9 were all made faster than M4 and M5 respectively, and this was a reasonable assumption after setting M4 and M5 as rate-determining. Reactions M7, M8, M10, and M11 were guessed for best fit, but could be ignored if M24 and M25 were made labile enough. M12 and M13 were derived from literature values.[24,27] Since rate of reaction was controlled by rate of formation of HOCl, M16 and M17 were set such that they were faster than M4 and M5. Kinetics parameters for reaction M20 were derived from this study, and subsequently, k_{M22} was made slightly faster than k_{M20}. Reactions M26 and M27 are known to be fast and nearly diffusion controlled, and they were

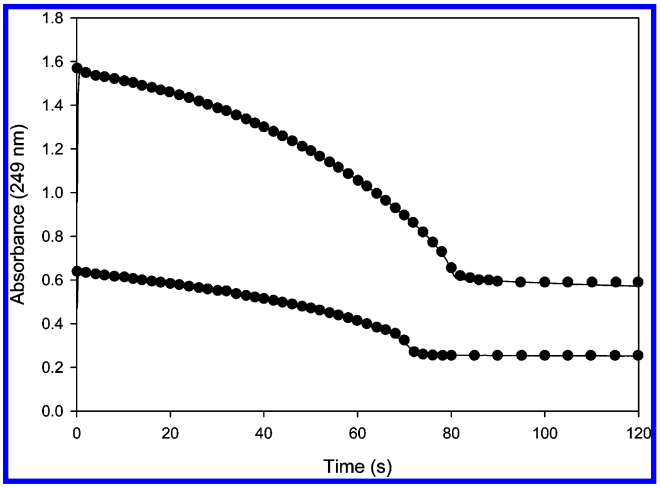

Figure 11. Simulations of the data shown in Figure 7C (traces b and e) using the mechanism in Table 2. Solid line: experimental; dots: simulation.

implemented thus. The autocatalytic reactions M14 and M15 were only relevant in low-to-medium acid concentrations. They were very important in determining the sigmoidal decay kinetics observed in Figure 7c. This model could adequately simulate Figures 2a, 3b, 6a, 7c, 9a, and 9b. While it could simulate the first part of Figure 8c, the uncertainties in the hydrolysis kinetics of the sulfinic and sulfonic acids made it difficult to simulate to second phase of that reaction. Figure 11 shows a simulations fit to the data shown in Figure 7c. These simulations showed that reactions M28 and M29 are extremely important in

accelerating the rate of consumption of PTU by rapidly forming ClO_2^- from ClO_2.

Conclusion

The oxidation of phenylthiourea is complicated by the formation of two stable intermediates: the sulfinic acid and the sulfonic acid on the pathway towards total desulfurization to form phenylurea. Its standard use as a goitrogenic must lie in its ability to abstract the iodine atom needed by the thyroid gland.[13] Its toxicity, however, must be derived from the deliberate cleavage of the C−S bond to yield highly reactive sulfur species that may interact with oxygen to yield reactive oxygen species. This appears to be a well-accepted route for the establishment of toxicities in thiocarbamides.[48,49] The physiological environment, which is slightly basic, destabilizes the oxo-acids in favor of the reduced sulfur species after cleavage of the C−S bond.[43,48]

Acknowledgment. We would like to acknowledge Gus Lawrence for synthesizing phenylthiourea dioxide. We would also like to thank Fungai Mukome for running ICPMS for us. This work was supported by Research Grant Numbers CHE 0137435, CHE 0341152, and CHE 0341769 from the National Science Foundation.

References and Notes

(1) Park, S. B.; Howald, W. N.; Cashman, J. R. *Chem. Res. Toxicol.* **1994**, *7*, 191−198.
(2) Del Corso, A.; Cappiello, M.; Mura, U. *Int. J. Biochem.* **1994**, *26*, 745−750.
(3) Organisciak, D. T.; Darrow, R. M.; Jiang, Y. I.; Marak, G. E.; Blanks, J. C. *Invest. Ophthalmol. Vis. Sci.* **1992**, *33*, 1599−1609.
(4) Olojo, R.; Simoyi, R. H. *J. Phys. Chem. A* **2004**, *108*, 1018−1023.
(5) Hodgson, E.; Levi, P. E. *Xenobiotica* **1992**, *22*, 1175−1183.
(6) Madan, A.; Parkinson, A.; Faiman, M. D. *Biochem. Pharmacol.* **1993**, *46*, 2291−2297.
(7) Hanzlik, R. P.; Cashman, J. R. *Drug Metab. Dispos.* **1983**, *11*, 201−205.
(8) Ziegler, D. M. *Annu. Rev. Pharmacol. Toxicol.* **1993**, *33*, 179−199.
(9) Guo, W. X.; Poulsen, L. L.; Ziegler, D. M. *Biochem. Pharmacol.* **1992**, *44*, 2029−2037.
(10) Poulsen, L. L.; Hyslop, R. M.; Ziegler, D. M. *Arch. Biochem. Biophys.* **1979**, *198*, 78−88.
(11) Smith, R. L.; Williams, R. T. *J. Med. Pharm. Chem.* **1961**, *4*, 97−107.
(12) Lee, P. W.; Arnau, T.; Neal, R. A. *Toxicol. Appl. Pharmacol.* **1980**, *53*, 164−173.
(13) Facchini, F.; Abbati, A.; Campagnoni, S. *Hum. Biol.* **1990**, *62*, 545−552.
(14) Bruck, R.; Frenkel, D.; Shirin, H.; Aeed, H.; Matas, Z.; Papa, M.; Zaidel, L.; Avni, Y.; Oren, R.; Halpern, Z. *Dig. Dis. Sci.* **1999**, *44*, 1228−1235.
(15) Kabadi, U.; Cech, R. *Thyroidology* **1994**, *6*, 87−92.
(16) Scott, A. M.; Powell, G. M.; Upshall, D. G.; Curtis, C. G. *Environ. Health Perspect.* **1990**, *85*, 43−50.
(17) Smith, R. L.; Williams, R. T. *J. Med. Pharm. Chem.* **1961**, *4*, 137−146.
(18) Indelli, A. *J. Phys. Chem.* **1964**, *68*, 3027−3031.
(19) Brauer, G. *Handbook of Preparative Organic Chemistry*; Academic Press: New York, 1963; p 301.
(20) Darkwa, J.; Olojo, R.; Chikwana, E.; Simoyi, R. H. *J. Phys. Chem. A* **2004**, *108*, 5576−5587.
(21) Doona, C. J.; Stanbury, D. M. *J. Phys. Chem.* **1994**, *98*, 12630−12634.
(22) Miller, A. E.; Bischoff, J. J.; Pae, K. *Chem. Res. Toxicol.* **1988**, *1*, 169−174.
(23) Epstein, I. R.; Kustin, K.; Simoyi, R. H. *J. Phys. Chem.* **1992**, *96*, 5852−5856.
(24) Horvath, A. K.; Nagypal, I.; Peintler, G.; Epstein, I. R.; Kustin, K. *J. Phys. Chem. A* **2003**, *107*, 6966−6973.
(25) Wang, L.; Margerum, D. W. *Inorg. Chem.* **2002**, *41*, 6099−6105.
(26) Jia, Z.; Margerum, D. W.; Francisco, J. S. *Inorg. Chem.* **2000**, *39*, 2614−2620.
(27) Peintler, G, Nagypal, I.; Epstein, I. R. *J. Phys. Chem.* **1990**, *94*, 2954−2960.
(28) Jones, J. B.; Chinake, C. R.; Simoyi, R. H. *J. Phys. Chem.* **1995**, *99*, 1523−1529.
(29) Salem, M. A.; Chinake, C. R.; Simoyi, R. H. *J. Phys. Chem.* **1996**, *100*, 9377−9384.
(30) Figlar, J. N.; Stanbury, D. M. *J. Phys. Chem. A* **1999**, *103*, 5732−5741.
(31) Darkwa, J.; Olojo, R.; Olagunju, O.; Otoikhian, A.; Simoyi, R. *J. Phys. Chem. A* **2003**, *107*, 9834−9845.
(32) Capozzi G.; Modena, G. *The chemistry of the thiol group*, 5th ed.; Wiley-Interscience: New York, 1974; pp 791−796.
(33) Hwang, E.; Cash, J. N.; Zabik, M. J. *J. Agric. Food Chem.* **2002**, *50*, 4734−4742.
(34) Chikwana, E.; Simoyi, R. H. *J. Phys. Chem. A* **2004**, *108*, 1024−1032.
(35) Furman, C. S.; Jia, Z. J.; Margerum, D. W. *Abstracts of Papers of the American Chemical Society* **1998**, *216*, U98.
(36) Kustin, K.; Eigen, M. *J. Am. Chem. Soc.* **1962**, *84*, 1355−1359.
(37) Taube, H.; Dodgen, H. *J. Am. Chem. Soc.* **1949**, *71*, 3330−3336.
(38) Nicoson, J. S.; Margerum, D. W. *Inorg. Chem.* **2002**, *41*, 342−347.
(39) Chinake, C. R.; Mundoma, C.; Olojo, R.; Chigwada, T.; Simoyi, R. H. *Phys. Chem. Chem. Phys.* **2001**, *3*, 4957−4964.
(40) Horvath, A. K.; Nagypal, I.; Epstein, I. R. *J. Phys. Chem. A* **2003**, *107*, 10063−10068.
(41) Horvath, A. K.; Nagypal, I. *J. Phys. Chem. A* **1998**, *102*, 7267−7272.
(42) Chinake, C. R.; Olojo, O.; Simoyi, R. H. *J. Phys. Chem. A* **1998**, *102*, 606−611.
(43) Makarov, S. V.; Mundoma, C.; Penn, J. H.; Svarovsky, S. A.; Simoyi, R. H. *J. Phys. Chem. A* **1998**, *102*, 6786−6792.
(44) Ojo, J. F.; Otoikhian, A.; Olojo, R.; Simoyi, R. H. *J. Phys. Chem. A* **2004**, *108*, 2457−2463.
(45) Makarov, S. V.; Mundoma, C.; Penn, J. H.; Petersen, J. L.; Svarovsky, S. A.; Simoyi, R. H. *Inorg. Chim. Acta* **1999**, *286*, 149−154.
(46) Datta, A. K.; Shi, X.; Kasprzak, K. S. *Carcinogenesis* **1993**, *14*, 417−422.
(47) Fabian, I.; Szucs, D.; Gordon, G. *J. Phys. Chem. A* **2000**, *104*, 8045−8049.
(48) Makarov, S. V.; Mundoma, C.; Svarovsky, S. A.; Shi, X.; Gannett, P. M.; Simoyi, R. H. *Arch. Biochem. Biophys.* **1999**, *367*, 289−296.
(49) Svarovsky, S. A.; Simoyi, R. H.; Makarov, S. V. *J. Phys. Chem. B* **2001**, *105*, 12634−12643.